1. MINERALOGY AND GEOCHEMISTRY OF ALKALI BASALTS FROM MAUD RISE, WEDDELL SEA, ANTARCTICA[1]

E. S. Schandl,[2] M. P. Gorton,[2] and F. J. Wicks[2,3]

ABSTRACT

Basalts from Maud Rise, Weddell Sea, are vesicular and olivine-phyric. Major, trace, and rare earth element concentrations are similar to those of alkali basalts from ocean islands and seamounts. The rocks are low in MgO, Cr, Ni, and Sc, and high in TiO_2, K_2O, P_2O_5, Zr, and LREE contents. The abundance of "primary" biotite and apatite in the matrix indicates the melting of a hydrous mantle. Prevalence of olivine and absence of plagioclase in the rocks suggests that the volatile in the melt was an H_2O-CO_2 mixture, where H_2O was < 0.5.

Mantle derived xenocrysts in the basalt include corroded orthopyroxene, chromite, apatite, and olivine. Olivine (Fo_{90}) is too magnesian to be in equilibrium with the basalts, as they contain only 5–6 wt% MgO.

Based on the presence of mantle xenocrysts, the high concentration of incompatible elements, the spatial and chemical affinity with other ocean island basalts from the area, and the relative age of the basalt (overlain by late Campanian sediments), it is suggested that Maud Rise was probably generated by hot-spot activity, possible during a ridge crest jump prior to 84 Ma (anomaly 34 time).

Iddingsite, a complex intergrowth of montmorillonite and goethite, is the major alteration product of second generation olivine. It is suggested that iddingsite crystallized at low temperatures (<200°C) from an oxidized fluid during deuteric alteration.

Vesicles are commonly filled by zeolites which have been replaced by K-feldspars.

INTRODUCTION

Tectonic Setting

The reconstruction of the tectonic evolution of the South Atlantic Ocean has been based on recognized seafloor magnetic anomalies, and has been a topic of considerable debate (Barker, 1979; LaBrecque and Hayes, 1979; Rabinowitz and LaBrecque, 1979; LaBrecque and Barker, 1981; Tucholke et al., 1981; Lawver et al., 1985; Martin and Hartnady, 1986; and Barker and Lawver, 1988). Although the various tectonic models differ in some detail, they all agree that seafloor spreading in the Southern Atlantic Oceans was accompanied by a series of ridge-jumps during the Mesozoic. These ridge jumps explain the shortening of the original 1400 km offset along the Agulhas-Falkland Fracture Zone. Ridge jumps have been proposed at 113 Ma, 93 Ma, and with greater consensus, at 60 to 64 Ma.

Maud Rise is an isolated topographic high in the Weddell Sea, and its tectonic history is believed to be related to the evolution of the Southern Atlantic Oceans. It has been suggested that Maud Rise was once part of the Agulhas Plateau but was separated from it during a ridge jump at 93 Ma (Martin and Hartnady, 1986). In this reconstruction of East Antarctica and South Africa, symmetry was observed between Mozambique Ridge-Astrid Ridge, Madagascar-Gunnerus Ridge and the Maud Rise-Agulhas Plateau pairs.

Maud Rise is located 700 km north of the Antarctic continent (Fig. 1). It is at an elevation 2000 m above the seafloor, and its crest is at 2080 m below sea level. Seven holes were drilled on the Rise during ODP Leg 113; four near the crest (Site 689) and three on the southwest flank (Site 690). Basalt was intersected in one hole at Site 690, at 317 mbsf. A 317 m thick sedimentary sequence of late Campanian age overlies the basaltic rocks (Barker, Kennett, et al., 1988).

As this was the first time basalt has been recovered from Maud Rise, it provides a unique opportunity to study basalts of unusual mineralogy and geochemistry from a new location in the Weddell Sea. The purposes of this study are threefold: (a) to characterize the mineralogy of basalts from Maud Rise; (b) to determine major, trace, and REE compositions, and use this information to deduce the source and environment that generated volcanism at Maud Rise; and (c) to discuss the significance of secondary minerals in the basalt.

Previous Work

Alkali basalts found in the Antarctic region include Kerguelen Island (Watkins et al., 1974), Kerguelen Plateau (Storey et al., 1988), the Antarctic Peninsula (Hole, 1988; Smellie, 1987); Ross Island, Antarctica, a part of the volcanic belt that parallels the Transantarctic Mountains (Goldich et al., 1975; Sun and Hanson, 1975), Bouvetoya Island (Imsland et al., 1977) and P-type basalts from several localities at and near the Bouvet triple junction (LeRoex et al., 1983). In addition, preliminary work suggests that some rocks drilled at northeast Georgia Rise during Leg 114 are probably transitional between alkali basalts and tholeiites (M. Perfit, pers. comm.).

ANALYTICAL METHODS

Whole rocks were analyzed for major and trace elements by X-ray fluorescence on-board ship during Leg 113, using the techniques described by Becker, Sakai, et al. (1988). Major elements were determined from fused beads and trace elements from pressed powder pellets. Trace element analyses were repeated on duplicate powder pellets at the Department of Geology, University of Toronto. Rare earth element compositions were determined by Instrumental Neutron Activation Analysis at the SLOWPOKE reactor, University of Toronto, using the procedures and analytical techniques described by Barnes and Gorton (1984).
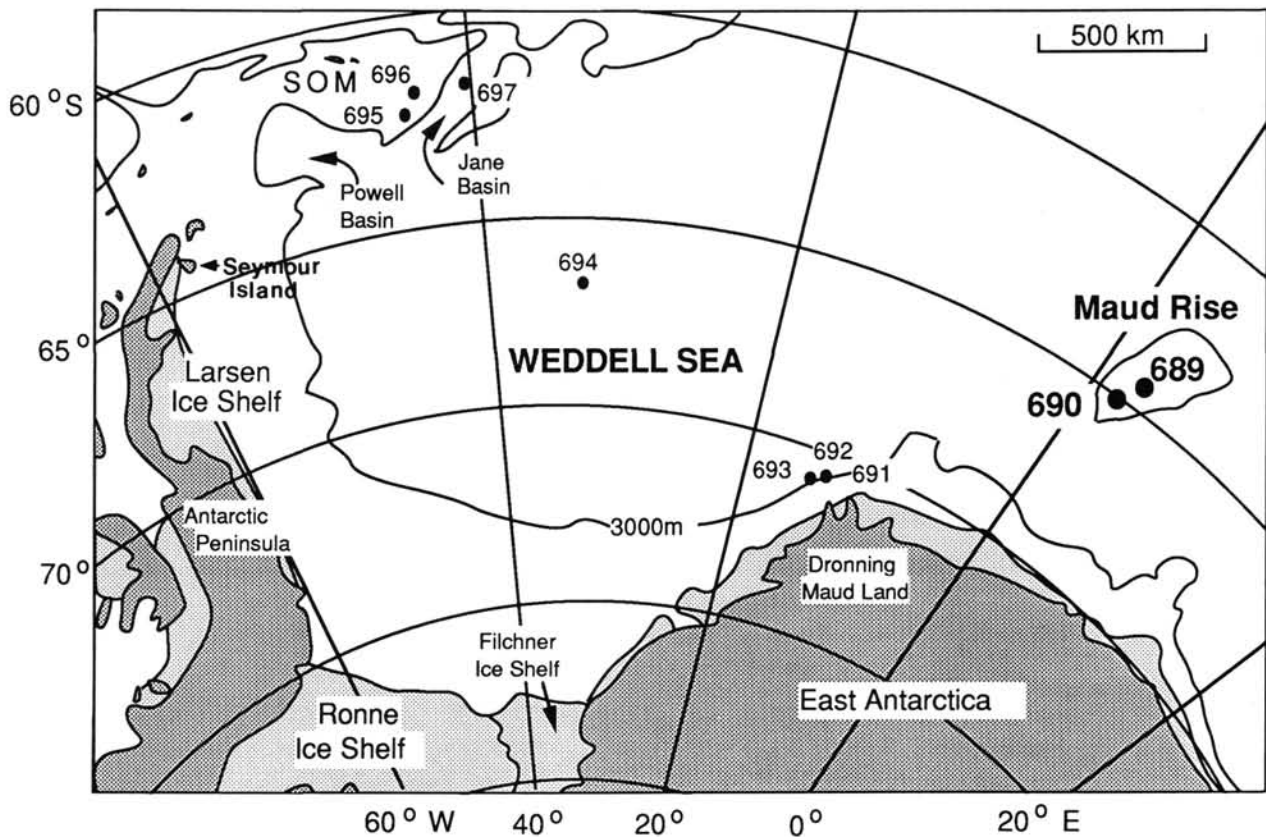
Figure 1. Location of Maud Rise; Leg 113 Sites 689, 690 in Weddell Sea (Barker, Kennett, et al., 1988).

The chemical composition of various minerals was determined by an ETEC electron microprobe, equipped with an energy dispersive system, at the Department of Geology, University of Toronto, and results are reported in Table 1. Composition of the glass was also determined by electron microprobe, and results are included in Table 2. Iddingsite was identified by X-ray powder diffraction using Cu K radiation in a 73 mm Debye Scherrer camera, at the Department of Mineralogy, Royal Ontario Museum.

TEXTURE AND MINERALOGY

The 2-m long drill core recovered at Site 690, Leg 113 contained two separate basalt flows, each approximately 1 m thick. The topmost 5 cm of each flow unit is glassy with perlitic texture (Pl. 1, Fig. 1). The main parts of the flows are dark grey, vesicular, and intensely fractured. The vesicles and fractures are filled with zeolites predominantly replaced by potassium feldspar, and calcite (Pl. 1, Fig. 2).

The basalts are olivine-phyric, and contain an abundance of olivine glomerocrysts in a matrix of fine-grained olivine, magnetite, ilmenite, biotite, and apatite. Two generations of olivine were recognized optically; fresh olivine represents the first generation. These are subhedral grains (up to 2 mm in size), having the composition of Fo_{90} (Table 1). A second generation of glomerocrysts, fine (<1 mm) anhedral to euhedral grains also occur as overgrowths, or as quench-textured coronas on xenocrysts of olivine and orthopyroxene, (Pl. 1, Figs. 3, 4), as well as small glomerocrysts. As the second generation olivine has been altered to iddingsite (Table 1), an intimate intergrowth of montmorillonite and goethite, its composition cannot be determined.

Apatites occur as acicular needles in the matrix, and some resemble quench-textured "hopper olivine" (Pl. 2, Fig. 1). Their composition is almost pure $CaO-P_2O_5$, with about 0.5% Cl (Table 1). Magnetite and ilmenite grains are blocky, needle or fern-shaped (Pl. 2, Fig. 2). Blocky magnetites are interstitial to the second-generation iddingsite altered olivine (Pl. 2, Fig. 3), and are often associated with pristine first generation olivine, whereas needles and fern-shaped grains constitute part of the matrix. Highly pleochroic (deep red-brown) radiating, needle-shaped biotite has nucleated from the basaltic glass (Pl. 2, Fig. 4). The chemical composition of Ti-rich biotite (TiO_2 = 4.7%) is shown in Table 1. As they are extremely fine-grained, a small component of the matrix glass may have been included in the analysis. Plagioclase is conspicuously absent from these basalts.

The rock matrix and the glassy tops are relatively fresh. Within the flow tops, olivine phenocrysts are altered mostly to calcite and less commonly to iddingsite (Pl. 3, Fig. 1). The glass also contains fine-grained blocky ilmenite. Below the glassy top, iddingsite appears as rod-like exsolution lamellae within olivine, and is speckled with interstitial magnetite. The color of iddingsite ranges from bright yellow to orange-red, and occasionally to bright green, but all are non-pleochroic.

The basalt contains a number of apatite, chromite, and orthopyroxene xenocrysts (Pl. 3, Figs. 2, 3, 4 and Pl. 1, Fig. 4). Their size ranges from 1 to 6 mm. All xenocrysts have resorbed grain boundaries, and are often subrounded. Apatite grains are difficult to recognize, as they are clouded with large numbers of inclusions. Orthopyroxene and olivine xenocrysts are rimmed by second generation olivine coronas now altered to iddingsite (Pl. 1, Figs. 3, 4). The chromite grains are rimmed by titanomagnetite. Occasional attached chromite and Mg-rich olivine grains (Pl. 3, Fig. 4) probably indicate a common source for both.

Orthopyroxene xenocrysts are enstatite, containing up to 5% Al_2O_3 (Table 1). Chromite xenocrysts are aluminum-rich, and contain up to 30% Al_2O_3. Chromite is rimmed by titaniferous

magnetite. The inner selvage of the rim has high Cr_2O_3 content (9.5%; Table 1), suggesting that this rim is not an overgrowth, but may have formed from reaction with the melt, via diffusion. Magnetite rims on chromites contain up to 16% TiO_2. Apatite xenocrysts in the basalt are anhedral, have cleavage traces and contain a large number of solid inclusions. Xenocrystic apatites are unusual in containing very high concentrations of Sr, La, Ce, Nd, and Sm (Table 1).

Vesicles and fractures in the basalt are filled with "zeolite" and calcite. The "zeolites" occur as fine to coarse-grained radiating bundles and predate calcite. Microprobe analysis shows that although their optical properties have been preserved, the zeolites have been completely replaced by feldspars (Table 1). The replacement of zeolites by potassium feldspar is not uncommon in ancient lakes, as demonstrated by the reaction:

$$NaAlSi_2O_6 \; H_2O + SiO_2 + K^+ \rightarrow KAlSi_3O_8 + H_2O + Na^+$$

analcime   potassium feldspar
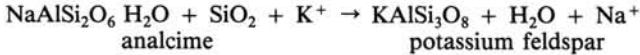
(Surdam 1977)

GEOCHEMISTRY

Eight samples were selected for major and trace element analyses, and results are shown in Table 2. Columns 1–4 represent the upper flow, and columns 4–8 the lower flow unit. Column 9 is the glass analysis from the top of the lower unit.

Major elements are reported on a volatile-free basis after ignition at 1000°C, and trace elements on a dried to 110°C basis. Due to the large number of vesicles and the small sample size, it

was not possible to separate vesicle-free samples for whole rock analysis. Therefore the glass was also analyzed for major elements by electron microprobe (Table 2). Two samples from each flow were analyzed for REE by INAA.

The Maud Rise basalts are characterized by low MgO content (4.0%–5.8%), high Al_2O_3 (14.6%), high P_2O_5 (1.7%) and high F/(F + M) ratio (0.63–0.7). The glass is enriched in Al_2O_3 (17.3%), Na_2O (6.5%), K_2O (6.5%), and is slightly depleted in MgO (3.5%) and FeO (7.3%) relative to the whole rock. Total alkalis in the glass are 12.5%.

The glass is much higher in alkalis, and lower in MgO than the whole rocks. Although the glass may have absorbed alkalis from seawater, it is more probable that the alkalis were lost from the whole rocks during alteration. MgO seems to be too low in both whole rocks and the glass, in view of Ni concentrations (119–184 ppm) and the abundance of olivine. Thus MgO may also have been modified.

Although samples for analysis were selected from core sections containing the least number of amygdules and fractures, it was not possible to separate completely vesicle-free samples for analysis. CaO concentrations are variable and high. The high CaO values are associated with low SiO_2 and high loss on ignition, and this is attributed to contamination by calcite. Then, in view of the above alterations, normative calculations are not thought to be meaningful.

Incompatible trace element abundances: Nb (77), Zr (500–600), Sr (921–1782), and Ba (859–1756); and the trace element ratios Zr/Y (18–19), Ti/Y (1094–1160), Nb/Y (2.6), La/Yb$_N$ (22), and Sr/Nb (20–22); are indicative of alkali basalts, al-

Table 1. Microprobe analysis of selected minerals from Maud Rise basalts, Hole 690C.

	OPX xenocrysts				Chromite xenocrysts				Olivine xenocrysts	
Sample	24X 42–46	24X 103–104	24X 103–104		24X 15–17	24X 15–17	24X 15–17		24X 42–46	24X 42–46
SiO_2	56.89	55.09	54.60	MgO	14.01	13.40	7.80	SiO_2	40.89	40.66
Al_2O_3	3.32	4.14	5.01	Al_2O_3	27.64	27.82	7.80	MgO	50.00	50.30
FeO	5.69	5.25	4.96	TiO_2	0.37	0.47	14.89	FeO	9.36	9.26
MgO	33.48	33.87	33.13	Cr_2O_3	32.14	31.05	9.50	NiO	0.25	0.35
CaO	1.28	1.11	1.12	FeO	23.63	24.50	55.67			
Cr_2O_3	nd	0.52	0.63	MnO	0.64	0.43	0.88			
Total	100.67	99.99	99.45	Total	98.42	97.67	94.25	Total	100.50	100.58

	Apatite				Biotite			Iddingsite	
Sample	24X 42–46 xenocryst	24X 42–46 xenocryst	24X 42–46 groundmass		24X 42–46	24X 42–46		24X 42–46	24X 42–46
CaO	55.55	55.86	53.69	SiO_2	42.90	43.47	SiO_2	37.27	36.71
P_2O_5	37.86	38.95	39.70	TiO_2	4.73	4.76	TiO_2	0.19	0.33
Cl	0.61	0.36	0.10	Al_2O_3	17.35	17.43	Al_2O_3	6.45	5.89
FeO	0.76	0.00	0.00	FeO	7.84	8.93	FeO	24.35	25.72
SrO	1.77	0.00	0.00	MgO	11.10	10.94	MgO	19.96	2.97
La_2O_3	0.00	0.72	0.00	CaO	1.19	2.14	CaO	0.85	0.85
Ce_2O_3	0.97	1.49	0.00	Na_2O	2.44	0.70	K_2O	0.94	0.56
Nd_2O_3	0.00	1.11	0.00	K_2O	7.26	6.59			
Total	97.53	98.49	93.49	Total	94.81	94.97	Total	90.02	92.05

	K-feldspar (cavity-filling)	
Sample	23X 15–17	23X 15–17
SiO_2	62.98	63.89
Al_2O_3	19.62	21.15
CaO	0.57	0.42
K_2O	12.73	11.31
Total	99.12	100.94

Note: Total Fe expressed as FeO. nd = not determined.

Table 2. Major and trace element analyses of basalts from Leg 113, Hole 690C.

Sample	23X 10–12	23X 52–53	24X 9–10	24X 15–17	24X 26–28	24X 64–67	24X 93–96	24X 119–121	Glass 15–17
SiO_2	48.73	47.36	48.55	47.53	45.44	45.49	45.10	44.86	48.70
TiO_2	3.39	3.34	3.57	3.50	3.29	3.37	3.30	3.30	3.60
Al_2O_3	14.63	14.94	15.25	14.99	14.34	14.53	14.40	14.63	17.30
FeO^t	10.10	9.75	10.19	10.42	9.64	9.84	9.85	9.48	7.30
MnO	0.12	0.12	0.11	0.12	0.11	0.38	0.12	0.12	0.00
MgO	5.75	4.02	4.99	5.06	5.21	4.57	4.51	4.40	3.50
CaO	8.34	11.68	7.78	8.28	12.41	11.89	12.85	15.93	6.00
Na_2O	2.84	2.64	3.06	2.95	2.53	2.93	2.86	2.57	6.50
K_2O	3.67	3.18	4.23	4.24	4.13	3.88	3.77	3.21	6.50
P_2O_5	1.80	1.75	1.63	1.73	1.78	1.72	1.67	1.80	nd
Total	99.36	98.85	99.36	98.82	98.88	98.60	98.43	99.65	98.00
LOI	6.8	9.9	7.8	7.6	10.5	11.9	9.3	13.5	nd
Nb	77	76	82	81	74	77	77	71	
Zr	542	535	571	562	516	542	533	500	
Y	29	29	32	32	28	30	28	28	
Sr	1544	1422	1543	1782	1591	1683	1449	921	
Rb	47	49	53	51	49	48	46	36	
Zn	180	137	140	142	192	135	130	120	
Cu	31	28	32	34	32	33	28	25	
Ni	184	119	136	129	141	128	139	130	
Cr	129	101	163	122	129	103	124	103	
V	150	158	173	162	158	173	166	157	
Ba	921	1062	1491	1478	1756	1122	859	675	
La	84.8			82.7	84.5			78.3	
Ce	167.0			194.0	165.0			176.0	
Nd	84.3			87.7	89.9			81.9	
Sm	14.7			14.3	14.7			13.9	
Eu	3.8			4.4	4.0			3.9	
Tb	1.4			1.5	1.5			1.4	
Yb	2.4			2.2	2.5			2.3	
Lu	0.37			0.27	0.30			0.31	
Sc	14.7			16.2	15.2			14.9	
Cs	0.5			0.8	0.4			0.7	
Th	4.6			4.9	4.9			4.6	
Hf	9.6			12.2	9.3			11.3	
Ta	4.6			5.3	5.8			4.6	

Note: FeO^t = total Fe expressed as FeO. nd = not determined.

though higher than the average alkali basalt (Frey et al., 1978; Wood et al., 1979; LeRoex, 1985; Hole, 1988). The Zr/Nb ratio of 7.0 however, is in agreement with alkali basalts in general.

Chondrite normalized REE plots of Maud Rise basalts and of typical Hawaiian alkali basalts (Frey, 1980) are shown on Figure 2. There is good correlation between the REE patterns from the two localities, confirming the alkalic composition of the basalts from Maud Rise.

When samples are plotted on the Ti-Zr-Y ternary diagram of Pearce and Cann (1973), the analyses lie on the "within plate basalt" area (Fig. 3). The Th/Yb (21) and Ta/Yb (2) ratios are consistent with within plate enrichment (Pearce, 1983).

Primordial mantle normalized multi element plots of incompatible elements of basalts from Bouvet, Tristan da Cunha, Ascension (Weaver et al., 1986), and Alexander Islands (Hole, 1988), and alkali basalts in general, show a trend of progressive increase from Y to Ta, a sharp decrease from Ta to Ce, and a pronounced peak at the Ta-Nb pair. Basalts from Maud Rise are broadly similar, but differ in having a relatively flat top on the plot between K and Ce for both localities, lacking the Ta-Nb peak, and having a strong Ba peak. These characteristics are similar to those of Gough Island (Fig. 4).

DISCUSSION

It was shown in the previous sections, that the chemistry of basalts from Maud Rise is similar to those of alkali basalts associated with ocean islands. What makes the Maud Rise basalts
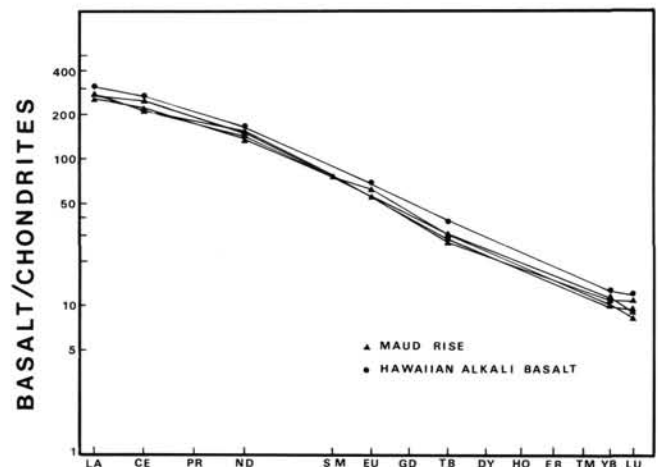

Figure 2. Chondrite normalized rare earth elements. Triangle = Maud Rise basalts, filled circle = Hawaiian alkali basalts (most highly enriched basalts from Frey, 1980).

unique is their very high enrichment in incompatible elements and LREE, their high vesicularity, and the absence of plagioclase. Other interesting features are the presence of mantle derived LREE-rich apatite, aluminous chromite, aluminous or-
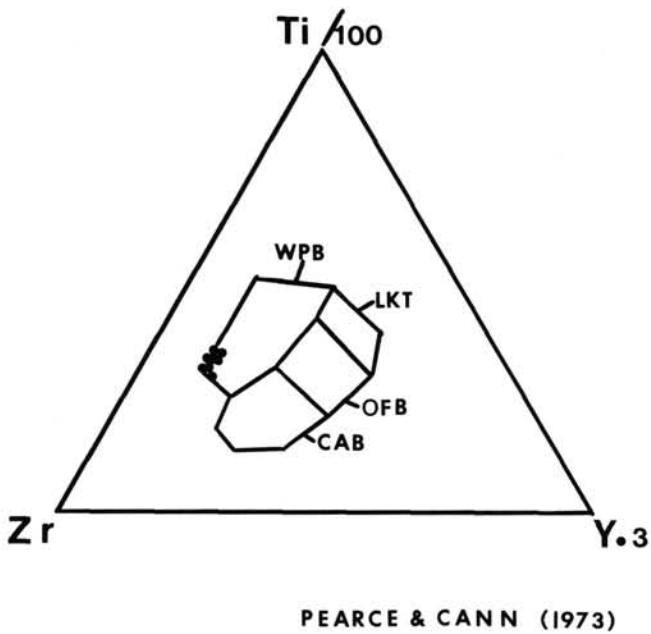
PEARCE & CANN (1973)

Figure 3. Ti-Zr-Y diagram of Pearce and Cann (1973). Filled circle = Maud Rise basalt. WPB = within plate basalt; OFB = ocean floor basalt; LKT = low K tholeiites; CAB = calc-alkalic basalt.

thopyroxene and forsteritic olivine xenocrysts; the pervasive alteration of olivine to iddingsite and of zeolites to potassium feldspars.

These features are discussed in the following section.

Geochemistry

Alkali basalts are believed to be derived directly from the mantle. In an oceanic environment they are most commonly associated with ocean islands and seamounts. They are typically undersaturated with respect to silica, and enriched in TiO_2, K_2O, P_2O_5, LREE, and other highly incompatible elements. According to Sun and Hanson (1975) and Fitton and Dunlop (1985), alkali basalts occurring in oceanic and continental environments are indistinguishable in their chemistry, as both originate from depths of about 60 km by a small degree of partial melting of a mantle previously enriched in incompatible elements.

Relatively high Nb/Y and Ti/Y ratios accompanied by low Zr/Nb and Ti/Nb ratios in basalts, are generally associated with low degrees of partial melting of a garnet bearing mantle source (Hole, 1988). This high concentration of incompatible elements is thought to be a function of mantle heterogeneity (enrichment of some regions), caused by the migration of a H_2O-CO_2 enriched supercritical fluid (Frey et al., 1978) below the LVZ. The enrichment, followed by low degree of partial melting then produces the trace and REE rich alkali basalts and basanites. Wood et al. (1979) suggested the enrichment of the mantle by 'veining' by small degree partial melts. Some investigators (Fitton and Dunlop, 1985) indicated that previous enrichment of the mantle is not necessary to produce the observed high concentrations of incompatible elements in alkali basalts. They invoked a mechanism analogous to zone refining, where rising magma leaches the LILE along grain boundaries. Based on detailed work on the Cameron line alkali basalts in west Africa, Fitton and Dunlop (1985) demonstrated that oceanic and continental alkali basalts are indistinguishable in their composition.

The basalts from Maud Rise are distinctive when compared to most "typical" ocean island basalts in the South Atlantic ocean, because of their high incompatible element ratios and concentrations. Only basalts from Gough Island are similar. It is suggested that both were derived by small degrees of partial melting of a previously enriched mantle. Double enrichment of the source region was proposed for the Gough Island lavas by LeRoex (1985), whereas Weaver et al. (1988) suggested the mixing of lava with ancient pelagic sediments, to explain the high La/Nb and Ba/Nb ratios.

One possible explanation for the relative enrichment of the Maud Rise basalts, as shown on the primordial mantle normalized plot (Fig. 4), is the melting of a fertile mantle clot, containing phlogopite and apatite at its source. The hydrous nature of the magma is evident from the abundance of vesicles and biotite in the basalt, and the melting of phlogopite can explain the high potassium content of the rock. It should be noted that the high concentration of La and Ce is accompanied by high concentrations of Sr and Nd, all of which are components of the mantle derived apatite xenocrysts (Table 1).

Absence of Plagioclase

Plagioclase is a normal component in the groundmass of alkali basalts. The Maud Rise basalts are unusual in lacking plagioclase.

Eggler (1973, 1974); Mysen and Boettcher (1975a, 1975b) and Burnham (1975) investigated the roles of volatiles on magma
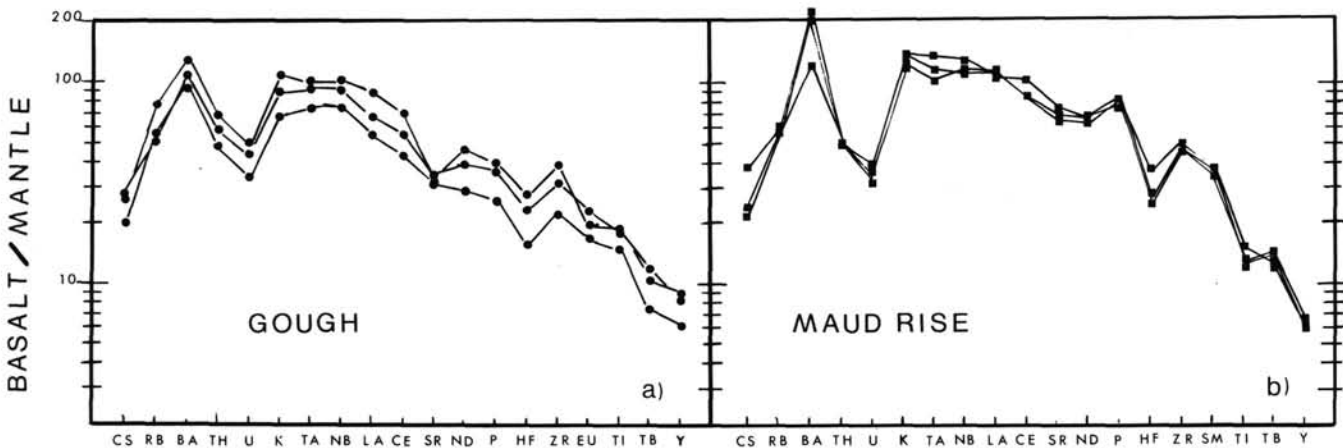

Figure 4. Incompatible elements normalized to mantle values. **A.** Gough Island (Weaver et al., 1986). **B.** Maud Rise.

generation and concluded that the composition of the volatiles in a magma plays a major role in controlling the minerals formed. In a H_2O-CO_2 mixture, with ratio of $H_2O > 0.5$, the sequence of crystallization will be, albite, orthoclase, anorthite, and quartz, and the rock will be quartz normative. If the volatile is CO_2 rich ($H_2O < 0.5$), forsterite, enstatite, and diopside will crystallize preferentially from the melt, and the rock will be nepheline-normative. Although normative mineralogy of the Maud Rise basalts cannot be calculated due to the abundance of vesicle-filling calcite and potassium feldspars (formed after zeolite), the absence of plagioclase and predominance of olivine indicates that the melt was CO_2 rich.

Mantle Xenocrysts

Partly resorbed xenocrysts of olivine, opx, chromite, and apatite are found in the Maud Rise basalts.

Olivine with composition Fo_{90} is not likely to be in equilibrium with any normal basalt (Roedder and Emslie, 1970). As these olivines occur with attached chromite they are probably xenocrystic.

Orthopyroxenes are enstatites which typically contain 4% Al_2O_3 and 0.5% Cr_2O_3. They are not in equilibrium with alkali basalts, and are presumably derived from the mantle.

The chromites are unusually aluminous and occasionally attached to Fo_{90} olivine, and are also thought to be mantle derived.

The Significance of Apatite Xenocrysts

There is some debate over the existence of residual apatite in the mantle (Beswick and Carmichael, 1978). As P_2O_5 is highly soluble in basic magmas, and the mantle has a relatively low concentration of P_2O_5 (200 ppm) (Sun and Nesbitt, 1977; Watson, 1980; Greenough, 1988; and Frey et al., 1982), apatite is not expected to be a residual phase in the mantle.

According to Watson (1980) apatite saturation in the Maud Rise basalts is not likely to occur until P_2O_5 reaches 3–4 wt%, thus we do not expect apatite phenocrysts. At the concentrations of 1.8% P_2O_5 observed, saturation will not occur until around 1000°C. This is consistent with the apatite needles observed in the groundmass, but not with the presence of xenocrysts.

A striking feature of the xenocrystic apatites is their high LREE contents. Ce_2O_3 contents are typically 1.4% (Table 1), which is equivalent to approximately 12,000 ppm. According to Watson and Green (1981), apatites crystallizing from these basalts would have Ce partition coefficients of about five. Thus, if the xenocrystic apatites crystallized from a basalt, the rock should have contained 2,400 ppm Ce to be in equilibrium with the apatites. This is more than ten times higher than the Ce content in the Maud Rise basalts, and higher than almost any liquids except kimberlites and carbonatites.

In view of the presence of other xenocrysts (opx, chromite and forsteritic olivine) of mantle origin, it is most likely that the apatites in the Maud Rise basalts were also derived from the mantle.

Vesicles in Basalts

Vesicularity in basalts is a reflection of the high volatile content of the magma. Moore et al. (1982) attributed the large number of vesicles in alkali basalts collected from the Loihi Seamount, Hawaii, to explosive volcanism. They suggested that during small degrees of partial melting of the mantle, volatiles can behave as incompatible elements, and partition into the liquid phase. In their samples, most alkali basalts contained a high proportion of vesicles (up to 50%), whereas the vesicle content of tholeiites from the same seamount was 2%–3%. The observations of Moore et al. (1982) can be applied to the basalts from Maud Rise, which are highly vesicular, and have alkalic compositions, implying that the magma was enriched in volatiles.

Iddingsite Alteration After Olivine

Rocks from Maud Rise do not show evidence of subaerial weathering. However, the replacement of olivine by iddingsite suggests an oxidizing environment during the alteration processes. Although a relatively common alteration product of basic volcanic rocks, the paragenesis of iddingsite is not well understood.

The name "iddingsite" describes complex intergrowths of montmorillonite and goethite (Baker and Haggerty, 1967). X-ray powder diffraction patterns of iddingsite from Maud Rise basalts indicate the presence of both minerals. There is considerable debate over the temperature of crystallization, and stability field of these minerals. It has been suggested (Fawcett, 1965) that iddingsite forms during high temperature deuteric alteration, and its presence is determined by the oxidation state of iron. But, as was pointed out by Baker and Haggerty (1967), the goethite in iddingsite preclude a high temperature origin, because the stability field of goethite is below 200°C.

The pseudomorphic replacement of olivine by iddingsite suggests that olivine crystallization was completed prior to alteration. Iddingsite is often found as rims on xenocrystic orthopyroxene and as rims on vesicles. It is absent from fracture selvages in the rocks, suggesting that fracturing in the rocks post-date iddingsite alteration. Therefore the fractures did not serve as conduits to iddingsite producing hydrothermal fluids. The pervasive alteration of olivine to iddingsite within the flow and predominantly to calcite on the flow tops suggest that iddingsite formed by deuteric alteration during cooling of the volcanic pile.

K-Feldspar Replacement of Zeolites

Vesicle and vein filling secondary minerals in the basalt are calcite and zeolite, although the latter has usually been replaced by K-feldspar. Textural evidence shows that the precipitation of zeolite in vesicles and fractures post-dated iddingsite alteration of olivine; vesicle walls are often lined with "zeolite" and filled by calcite. The "zeolites" have the appearance, textures, and optical orientation typical of cavity-filling zeolites, but microprobe analyses (Table 1) usually identifies them as K-feldspars.

Hot hydrothermal fluids circulating through a basaltic pile tend to precipitate sodium-rich zeolites. In an alkalic system, such as the alkali basalts at Maud Rise, zeolites in the vesicles will dissolve with decreasing temperature, and the fluid will precipitate potassium feldspars (R. Martin, pers. comm.). It is not necessary to have particularly saline solutions for this transformation to take place.

CONCLUSIONS

The basalt at Maud Rise was derived from a hydrous part of the mantle, which was enriched in incompatible elements. The preferential crystallization of olivine and the lack of plagioclase suggests that volatiles in the melt were a mixture of H_2O-CO_2, where CO_2 was the dominant volatile species.

Due to the small basalt recovery, we can only speculate at present as to the tectonic link between Maud Rise and other alkali basalt-bearing localities in the South Atlantic Ocean. Some basalts sampled along the Bouvet fracture zone (LeRoex et al., 1983), Tristan da Cunha Island (Weaver et al., 1987), Alexander Island (Hole, 1988), Gough Island (LeRoex, 1985), Kerguelen Island (Watkins et al., 1974), and Kerguelen Plateau (Schliech, Wise Jr., et al., 1988) bear chemical resemblance to the basalts from Maud Rise, as do others from various ocean islands and seamounts on the global scale. However, there are also differences as well. Basalts from Maud Rise have generally higher concentrations and ratios of incompatible elements than alkali basalts from the above localities, except for Gough Island.

The presence of mantle xenocrysts and the high concentration of incompatible elements suggests that the Maud Rise basalt was derived from a previously enriched mantle source by a small degree of partial melting of garnet lherzolite, where phlogopite and apatite were minor phases, and that Maud Rise was probably generated by hot-spot activity away from the mid-ocean ridge axis or possibly in association with a ridge jump, before 84 Ma. That the 2 m long drill core contains two flow tops suggests that these thin flows represent the waning stages of alkalic volcanism.

ACKNOWLEDGMENTS

REFERENCES

Baker, I., and Haggerty, S. E., 1967. The alteration of olivine in basaltic and associated lavas. Part II. Intermediate and low temperature alteration. *Contrib. Mineral. Petrol.*, 16:258–273.

Barker, P. F., 1979. The history of ridge crest offset at the Falkland-Agulhas Fracture Zone from a small circle geophysical profile. *Geophys. J. R. Astron. Soc.*, 59:131–145.

Barker, P. F., Kennett, J. P., et al., 1988. *Proc. ODP Init. Repts.*, 113: College Station, TX (Ocean Drilling Program).

Barker, P. F., and Lawver, L. A., 1988. South American-Antarctic Plate Motion over the past 50 Myr, and the evolution of the South American-Antarctic ridge. *Geophys. J.*, 94:377–386.

Barnes, Sarah-Jane, and Gorton, M. P., 1984. Trace Element Analysis by Neutron Activation With a Low Flux Reactor (Slowpoke—II): Results for International Reference Rocks. *Geostandards News.*, 8: 17–23.

Becker, K, Sakai, H., et al., 1988. *Proc. ODP Init. Repts.* 111: College Station, TX (Ocean Drilling Program).

Beswick, A. E., and Carmichael, I.S.E., 1978. Constraints on mantle source compositions imposed by phosphorus and the Rare-Earth Elements. *Contrib. Mineral. Petrol.*, 67:317–330.

Burnham, C. W., 1975. Water and magmas: a mixing model. *Geochim. Cosmochim. Acta.*, 39:1077–1084.

Eggler, D. H., 1973. Role of CO_2 in melting processes in the mantle. *Carn. Inst. Wash. Yearb.*, 72:457–467.

————, 1974. Effect of CO_2 on melting of peridotite. *Carn. Inst. Wash. Yearb.*, 73:415–224.

Fawcett, J. J., 1965. Alteration products of olivine and pyroxene in basalt lavas from the Isle of Mull. *Mineral. Mag.*, 35:55–68.

Fitton, J. G., and Dunlop, H. M., 1985. The Cameroon line, West Africa, and its bearing on the origin of oceanic and continental alkali basalt. *Earth Planet. Sci. Lett.*, 72:23–38.

Frey, F. A., 1980. Applications of Neutron activation analysis in mineralogy and petrology. *In* Muecke, G. K., (Ed.), *Neutron Activation Analysis in the Geosciences, Short Course Notes.* Geol. Assoc. Can/Mineral. Assoc. Can.,Halifax, 167–210.

Frey, F. A., Green, D. H., and Roy, S. D., 1978. Integrated model of basalt petrogenesis: A study of quartz tholeiites to olivine melilitites from South Eastern Australia utilizing geochemical and experimental petrological data. *J. Petrol.*, 19:463–513.

Goldich, S. S., Treves, S. B., Suhr, N. H., and Stuckless, J. S., 1975. Geochemistry of the Cenozoic volcanic rocks of Ross Island and vicinity, Antarctica. *J. Geol.*, 83:415–435.

Greenough, J. D., 1988. Minor phases in the Earth's mantle: Evidence from trace and minor element patterns in primitive alkaline magmas. *Chem. Geol.*, 69:177–192.

Hole, M. J., 1988. Post-subduction alkaline volcanism along the Antarctic Peninsula. *J. Geol. Soc.*, London, 145:985–998.

Imsland, P., Larsen, J. G., Prestwick, T., and Sigmond, E., 1977. The geology and petrology of Buovetoya, South Atlantic Ocean. *Lithos*, 10:213–34.

LaBrecque, J. L., and Barker, P. F., 1981. The age of the Weddell Sea. *Nature*, 290:489–492.

LaBrecque, J. L., and Hayes, D. E., 1979. Seafloor spreading history of the Agulhas Basin. *Earth Planet. Sci. Lett.*, 45:411–428.

Lawver, L. A., Sclater, J. G., and Meinke, L., 1985. Mesozoic and Cenozoic reconstruction of the South Atlantic. *Tectonophysics*, 114: 233–254.

LeRoex, A. P., 1985. Geochemistry, Mineralogy and Magmatic Evolution of the Basaltic and trachytic Lavas from Gough Island, South Atlantic. *J. Petrol.*, 26:149–186.

LeRoex, A. P., Dick, H.J.B., Erlank, A. J., Reid, A. M., Frey, F. A., and Hart, S. R., 1983. Geochemistry, Mineralogy and petrogenesis of lavas erupted along the southwest Indian Ridge between the Bouvet triple junction and 11 degrees east. *J. Petrol.*, 24:267–318.

Martin, A. K., and Hartnady, C.J.H., 1986. Plate tectonic development of the South West Indian Ocean: A revised reconstruction of East Antarctica and Africa. *J. Geophys. Res.*, 91, B5:4767–4786.

Moore, J. G, Clague, D. A., and Normark, W. R., 1982. Diverse basalt types from Loihi seamount, Hawaii. *Geology*, 10:88–92.

Mysen, B. O., and Boettcher, A. L., 1975a. Melting in a hydrous mantle: l, Phase relations of natural peridotite at high pressures and temperatures with controlled activities of water, carbon dioxide and hydrogen. *J. Petrol.*, 16:520–548.

————, 1975b. Melting of a hydrous mantle: II. Geochemistry of crystals and liquids formed by anatexis of mantle peridotite at high pressures and temperatures as the function of controlled activities of water, hydrogen and carbon dioxide. *J. Petrol.*, 16:549–593.

Pearce, J. A., 1983. Role of the sub-continental lithosphere in magma genesis at active continental margins. *In* Hakesworth, C. J. and Norry, M. J. (Eds.), *Continental Basalts and Mantle Xenoliths.* Shiva Publishing Ltd., 230–249.

Pearce, J. A., and Cann, J. R., 1973. Tectonic setting of basic volcanic rocks determined, using trace element analyses. *Earth Planet. Sci. Lett.*, 19:290–300.

Rabinowitz, P. D., and LaBrecque, J. L., 1979. The Mesozoic South Atlantic Ocean and evolution of its continental margins. *J. Geophys. Res.*, 84:5973–6002.

Roeder, P. L., and Emslie, R. F., 1970. Olivine-liquid equilibrium. *Contrib. Mineral. Petrol.*, 29:279–285.

Schliech, R., Wise Jr., S. W., et al., 1988. That sinking feeling. *Nature*, 334:385–386.

Smellie, J. L., 1987. Geochemistry and tectonic setting of Cenozoic alkali basalts from Alexander Island, Antarctic Peninsula. *J. Volcanol. Geotherm. Res.*, 32:269–285.

Storey, M., Saunders, A. D., Tarney, J., Leat, P., Thirlwall, M. F., Thompson, R. N., Menzies, M. A., and Marriner, G. F., 1988. Geochemical evidence for plume-mantle interactions beneath Kerguelen and Heard Islands, Indian Ocean. *Nature*, 336:371–374.

Sun, S. S., and Hanson, G. N., 1975. Origin of Ross Island Basanitoids and limitations upon the heterogeneity of mantle sources for alkali basalts and nephelinites. *Contrib. Mineral. Petrol.*, 52:77–106.

Sun, S. S., and Nesbitt, R. W., 1977. Chemical heterogeneity of the Archean mantle, composition of the earth and mantle evolution. *Earth Planet. Sci. Lett.*, 35:429–448.

Surdam, R. C., 1977. *In* Mumpton, F. A. (Ed.), *Zeolites in closed hydrologic systems.* Mineral. Soc. Am. Short Course Notes, 4:65–91.

Tucholke, B. E., Houtz, R. E. and Barrett, D. M., 1981. Continental crust beneath the Agulhas Plateau, Southwest Indian Ocean. *J. Geophys. Res.*, 86:3791–3806.

Watkins, N. D., Gunn, B. M., Nougier, J., and Baksi, A. K., 1974. Kerguelen: Continental fragment or oceanic island? *Geol. Soc. Am. Bull.*, 85:201–212.

Watson, E. B., 1980. Apatite and phosphorus in mantle source regions: an experimental study of apatite/melt equilibria at pressures to 25 kb. *Earth Planet. Sci. Lett.*, 51:322–335.

Watson, E. B., and Green, T. H., 1981. Apatite/liquid partition coefficients for the rare earth elements and strontium. *Earth Planet. Sci. Lett.*, 56:405–421.

Weaver, B. L., Wood, D. A., Tarney, J., and Joron, J. L., 1986. Role of subducted sediment in the genesis of ocean island basalts: geochemical evidence from South Atlantic Ocean islands. *Geology*, 14:275–278.

Wood, D. A., Joron, J. L., Treuil, M., Norry, M., and Tarney, J., 1979. Elemental and Sr isotope variations in basic lavas from Iceland and the surrounding ocean floor. *Contrib. Mineral. Petrol.*, 70:319–339.
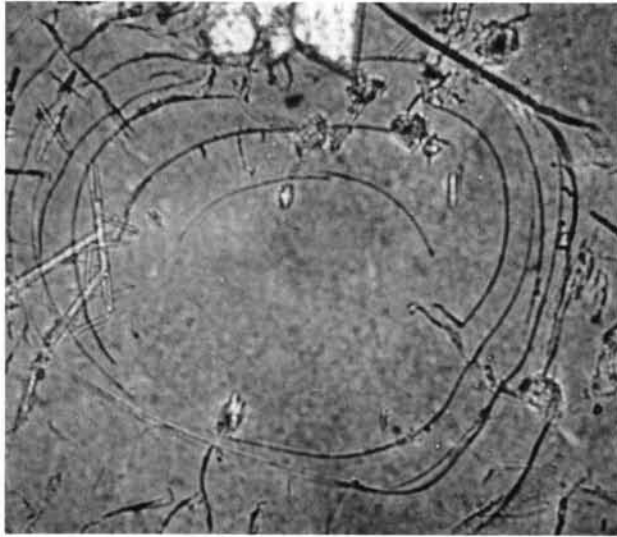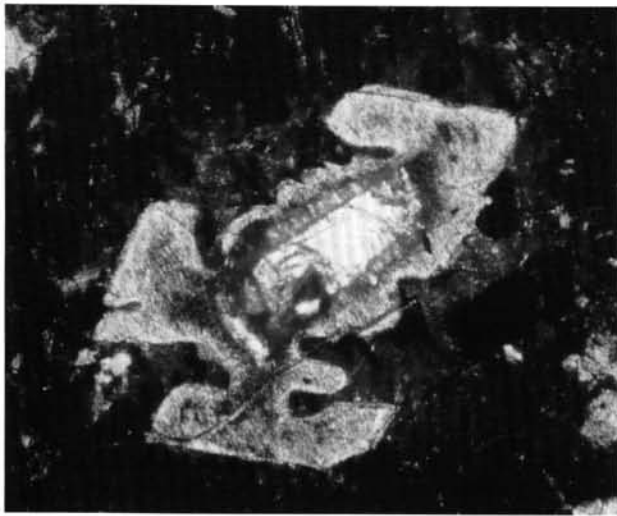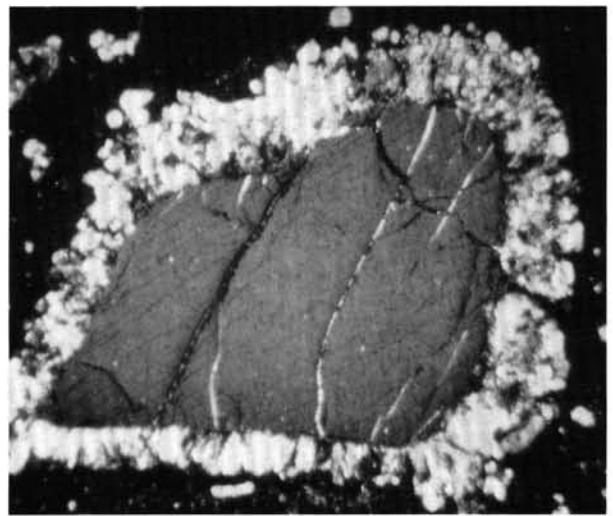
Plate 1.   **1.** Perlite in glassy flow top; upper flow, Ppl., Sample 113-690C-23X-1, 4–6 cm. Scale bar = 0.5 mm.   **2.** Vesicles and fractures, filled with zeolite and calcite in basalt core, Sample 113-690C-24X-1, 46–59 cm.   **3.** Olivine xenocryst (Fo$_{90}$) overgrown by second generation quench textured olivine corona, now altered to iddingsite, XN, Sample 113-690C-23X-1, 4–6 cm. Scale bar = 0.5 mm.   **4.** Orthopyroxene xenocryst rimmed by second generation olivine, now altered to iddingsite, XN, Sample 113-690C-24X-1, 16–18 cm. Ppl = plane polarized light; XN = crossed polars. Scale bar = 1 mm.
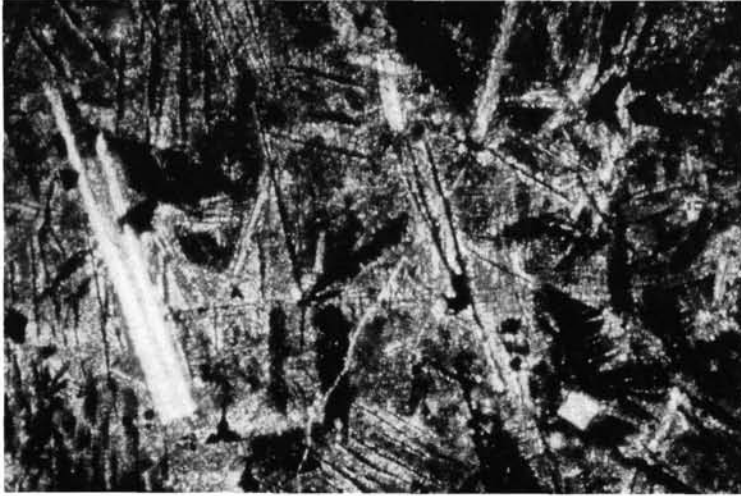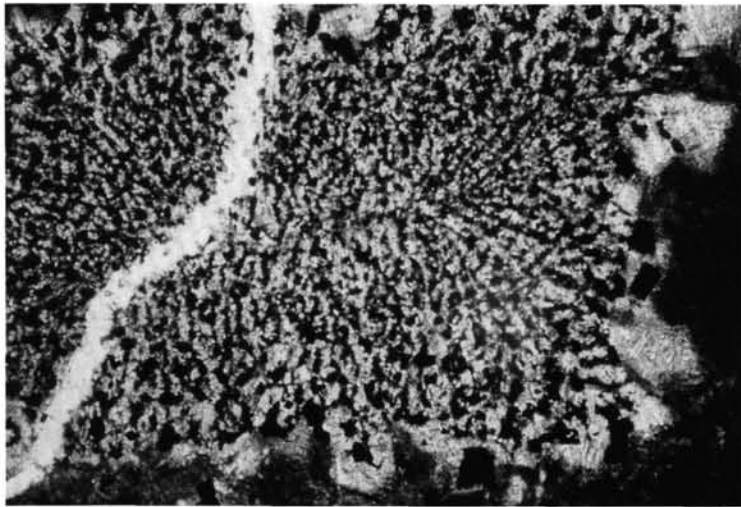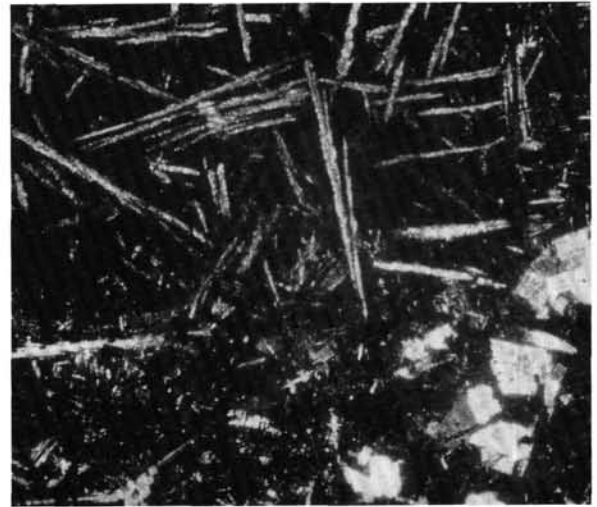
Plate 2. **1.** Quench textured, "hopper olivine" shaped apatite in basalt matrix, Ppl., Sample 113-690C-24X-1, 111–113 cm. Scale bar = 0.2 mm. **2.** Fern and needle shaped magnetite, Ppl., Sample 113-690C-24X-1, 111–113 cm. Scale bar = 0.5 mm. **3.** Blocky magnetite interstitial to olivine aggregate now altered to iddingsite, Ppl., Sample 113-690C-24X-1, 42–46 cm. Scale bar = 0.5 mm. **4.** Biotite needles nucleate from glass, and glomerocrysts of olivine are altered to iddingsite, XN., Sample 113-690C-24X-1, 16–18 cm. Ppl = plane polarized light; XN = crossed polars. Scale bar = 0.5 mm.
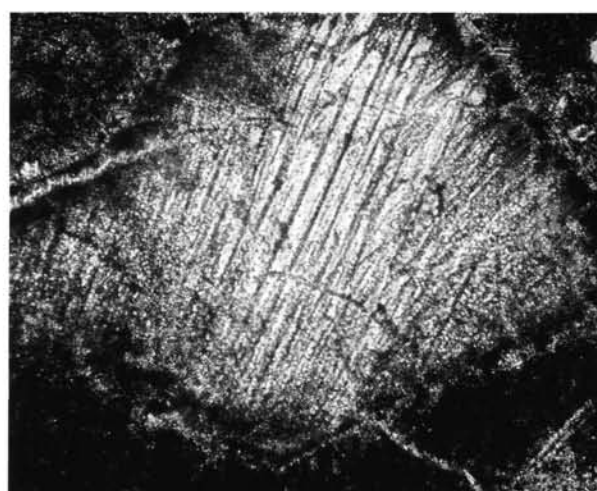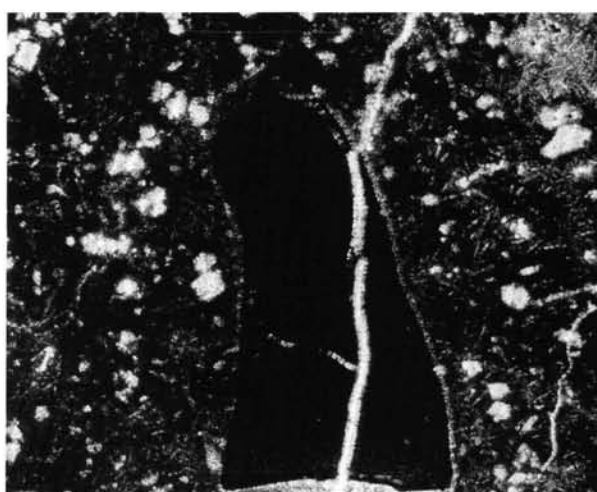
Plate 3. **1.** Olivine glomerocrysts altered to calcite, XN., Sample 113-690C-23X-1, 4–6 cm. Scale bar = 0.2 mm. **2.** Apatite xenocryst with cleavage traces, XN., Sample 113-690C-24X-1, 42–46 cm. Scale bar = 0.5 mm. **3.** Olivine xenocryst attached to chromite xenocryst (rimmed by titaniferous magnetite), and small olivine glomerocrysts are altered to iddingsite, Ppl., Sample 113-690C-24X-1, 111–113 cm. Scale bar = 0.5 mm. **4.** Chromite xenocryst rimmed by titaniferous magnetite, and cross-cut by zeolite vein, XN, Sample 113-690C-24X-1, 15–17 cm. Ppl = plane polarized light; XN = crossed polars. Scale bar = 1.0 mm.